frontiers | Frontiers in Chemistry

TYPE Original Research
PUBLISHED 07 September 2022
DOI 10.3389/fchem.2022.991625

OPEN ACCESS

EDITED BY
Hans-Conrad zur Loye,
University of South Carolina,
United States

REVIEWED BY
Arthur Mar,
University of Alberta, Canada
Boniface Fokwa,
University of California, Riverside,
United States

*CORRESPONDENCE
Svilen Bobev,
bobev@udel.edu

SPECIALTY SECTION
This article was submitted to Inorganic Chemistry,
a section of the journal
Frontiers in Chemistry

RECEIVED 11 July 2022
ACCEPTED 10 August 2022
PUBLISHED 07 September 2022

CITATION
Peng W, Baranets S and Bobev S (2022), Synthesis, crystal and electronic structure of $BaLi_xCd_{13-x}$ (x ≈ 2). *Front. Chem.* 10:991625. doi: 10.3389/fchem.2022.991625

Synthesis, crystal and electronic structure of $BaLi_xCd_{13-x}$ ($x \approx 2$)

Wanyue Peng, Sviatoslav Baranets and Svilen Bobev*

Department of Chemistry and Biochemistry, University of Delaware, Newark, DE, United States

A new ternary phase has been synthesized and structurally characterized. $BaLi_xCd_{13-x}$ ($x \approx 2$) adopts the cubic $NaZn_{13}$ structure type (space group $Fm\overline{3}c$, Pearson symbol *cF*112) with unit cell parameter a = 13.5548 (10) Å. Structure refinements from single-crystal X-ray diffraction data demonstrate that the Li atoms are exclusively found at the centers of the Cd_{12}-icosahedra. Since a cubic $BaCd_{13}$ phase does not exist, and the tetragonal $BaCd_{11}$ is the most Cd-rich phase in the Ba–Cd system, $BaLi_xCd_{13-x}$ ($x \approx 2$) has to be considered as a true ternary compound. As opposed to the typical electron count of ca. 27*e*-per formula unit for many known compounds with the $NaZn_{13}$ structure type, $BaLi_xCd_{13-x}$ ($x \approx 2$) only has ca. 26*e*-, suggesting that both electronic and geometric factors are at play. Finally, the bonding characteristics of the cubic $BaLi_xCd_{13-x}$ ($x \approx 2$) and tetragonal $BaCd_{11}$ are investigated using the TB-LMTO-ASA method, showing metallic-like behavior.

KEYWORDS

Cd, Li, single-crystal X-ray diffraction, crystal structure, synthesis

1 Introduction

In recent papers, we described new results from our exploratory work in the Ba–Li–In–Ge (Ovchinnikov and Bobev, 2019) and Ba–Li–Cd–Ge systems (Baranets et al., 2021b). As noted therein, our synthetic approach employed molten In and Cd as metal fluxes, allowing us to grow crystals of the quaternary phases, $BaLi_{2+x}In_{2-x}Ge_2$ ($0 \leq x \leq 0.66$) and $BaLi_2Cd_2Ge_2$ ($CaCu_4P_2$ type, space group $R\overline{3}m$; Pearson code *hR*7). The structure of this indium-germanide was found to respond to small changes in the chemical composition (alterations of the Li/In ratio) by virtue of cleaving homoatomic In–In bonding (Ovchinnikov and Bobev, 2019). $BaLi_2Cd_2Ge_2$ (Baranets et al., 2021), on the other hand, was found to be less flexible as far as the structure is concerned, just like its quaternary $BaMg_2Li_2Ge_2$ analog (Zürcher et al., 2001). On this note, it is instructive to mention that despite the resemblance between the chemical compositions, and structures of $BaMg_2Li_2Ge_2$ and $BaLi_2Cd_2Ge_2$ as compared to $BaLi_{2+x}In_{2-x}Ge_2$, all three phases show subtly different bonding characteristics. The differences are most pronounced between the structures with trivalent In vs. those with divalent Mg and Cd (Zürcher et al., 2001; Ovchinnikov and Bobev, 2019; Baranets et al., 2021b), attesting to the importance of the valence electron count for the peculiarities of each structure.

Cadmium metal is known to have considerable toxicity with a destructive impact on most living systems. Due to its low boiling point, Cd is also far from an ideal solvent for

high-temperature reactions. However, the crucial role of Cd in the flux growth of new intermetallic compounds makes the current study fit into this special issue on *Crystal Growth Under Extreme Conditions*. $BaLi_2Cd_2Ge_2$ (Baranets et al., 2021) together with Yb_2CdSb_2 (Xia and Bobev, 2007a), Sr_2CdAs_2 (Wang et al., 2011), Ba_2CdAs_2 (Wang et al., 2011), Eu_2CdAs_2 (Wang et al., 2011), $Ba_{11}Cd_8Bi_{14}$ (Xia and Bobev, 2006a), RE_2CdGe_2 (*RE* = Pr, Nd, Sm, Gd–Yb; Y) (Guo et al., 2012), $Ba_2Cd_3Bi_4$ (Xia and Bobev, 2006b), $A_{14}Cd_{1+x}Pn_{11}$ ($0 \le x \le 0.3$; *A* = Sr, Eu; *Pn* = As, Sb) (Makongo et al., 2015), $Sr_3Cd_8Ge_4$ (Suen et al., 2018), $Eu_3Cd_8Ge_4$ (Suen et al., 2018), and $Eu_{10}Cd_6Bi_{12}$ (Xia and Bobev, 2007b) from our laboratory have come into being by employing molten Cd as a flux for the synthesis. This is also the case with the title compound, $BaLi_xCd_{13-x}$ ($x \approx 2$). As mentioned above, $BaLi_xCd_{13-x}$ ($x \approx 2$) was serendipitously obtained during the exploratory work in the *AE*–Li–Cd–Si and *AE*–Li–Cd–Ge systems (*AE* = alkaline earth metals Ca, Sr, Ba, and the nominally divalent Eu, Yb). As a result of such work, the new cubic $BaLi_xCd_{13-x}$ ($x \approx 2$) phase was discovered. It is the first structurally characterized compound between the respective elements and crystallizes with the common $NaZn_{13}$ structure type (space group $Fm\bar{3}c$, Pearson symbol *cF*112). Yet, a binary phase $BaCd_{13}$ with this structure is unknown, making $BaLi_xCd_{13-x}$ ($x \approx 2$) a true ternary compound.

The crystal growth from Cd flux, the structural characterization, as well as a brief analysis of the chemical bonding of $BaLi_xCd_{13-x}$ ($x \approx 2$) and $BaCd_{11}$ are the main subject of discussion in this paper.

2 Materials and methods

2.1 Synthesis

The starting materials were purchased from Alfa Aesar, all with stated purity of 99.9 wt% or better. The metals were stored in an argon-filled glovebox and used as received. The surface of the Li rod was cleaned with a scalpel blade prior to cutting and using it.

Single crystals were synthesized *via* the flux growth method. As stated already, reactions aimed at $AELi_2Cd_2Ge_2$ (*AE* = alkaline-earth metal) were the starting point for this research, (Baranets et al., 2021b), and the title compound $BaLi_xCd_{13-x}$ ($x \approx 2$) was identified as a minor side product of such experiment. Subsequently, the samples were prepared without Ge in the elemental mixtures, where excessive stoichiometric amounts of Cd served as the flux for all compositions. A starting composition of Ba:Li:Cd: of 1:12:20 was used for $BaLi_xCd_{13-x}$ ($x \approx 2$). The 6-fold excess Li was chosen due to its high vapor pressure and losses at the reaction temperature. The corresponding amounts of elements (Ba rod, Cd shot, Zn shot, Ca shot, Yb shot, Li rod) were loaded into alumina crucibles. A piece of quartz wool was placed at the bottom of a fused silica ampoule. The alumina crucible was then loaded to the bottom of an ampoule. Another piece of quartz wool was placed on top of the crucible without touching the elements inside. The ampoules were sealed under a vacuum level of ca. 30 millitorr.

All the samples in this study were heated in muffle furnaces with a temperature profile as the following: 100°C → 20°C/h to 200°C → 50°C/h to 700°C → held at 700°C for 12.5 h → 4°C/h to 550°C. At this point of the crystal growth, the sealed tube was taken out from the furnace, flipped, and the molten metallic flux was separated from the grown crystals by centrifugation. After that, the sealed ampoule was brought in the glovebox and break-opened. Inspection of the specimen under an optical microscope revealed the presence of many small, grey crystals with a metallic luster, usually clustered together. Single-crystal X-ray diffraction confirmed them to be the new cubic $BaLi_xCd_{13-x}$ ($x \approx 2$) phase. A portion of the crystallites was then ground into fine powders with a mortar and pestle for powder X-ray diffraction, attesting the presence of the cubic phase in the bulk. The experiment was repeated in a Nb-tube to confirm that the results are repeatable in both alumina and Nb containers. Such reactions also verified that no inadvertent reduction of the Al_2O_3 can become a source of Al metal, as experienced recently by us in another materials system (Baranets and Bobev, 2021a).

Following the structure elucidation of $BaLi_xCd_{13-x}$ ($x \approx 2$), reactions aimed at $AELi_xCd_{13-x}$ ($x \approx 2$) (*AE* = Ca, Sr, Eu, Yb) were set up with the same nominal compositions as the ones described in the preceding paragraph, but they were unsuccessful. An attempt to grow crystals from Cd-flux reaction but without Li in the nominal mixture resulted in the growth of the known binary phase $BaCd_{11}$ (Sanderson and Baenziger, 1953). Since its structure has not been refined from single-crystal X-ray diffraction data and since the quality of the obtained crystals was excellent, herein we supply this information as well.

Crystals of $BaLi_xCd_{13-x}$ ($x \approx 2$) do not appear to degrade in air over a period of 1 week. Powder X-ray diffraction patterns also show the polycrystalline material to be air- and moisture-stable for the same amount of time and possibly even longer.

2.2 Powder X-ray diffraction and single-crystal X-ray diffraction

The X-ray powder diffraction patterns were collected using a Rigaku Miniflex powder diffractometer utilizing Ni-filtered Cu K_α radiation (λ = 1.5418 Å) and were used for phase identification only. All additional structural work was done using single-crystal X-ray diffraction methods.

Single-crystal X-ray diffraction measurements (SC-XRD) were performed using a Bruker APEX II diffractometer with monochromated Mo Kα radiation. Single crystal geometries are typically in block shape, with each side smaller than 60 μm in length. Crystals were selected under a microscope in dry

TABLE 1 Selected crystallographic data and structure refinement parameters for $BaLi_xCd_{13-x}$ ($x \approx 2$).

Formula	$BaLi_{2.14(4)}Cd_{10.86}$
Formula Weight/g mol^{-1}	1,373.0
Radiation, λ	Mo K_α, 0.71073 Å
Temperature/K	200 (2)
Crystal system	Cubic
Space Group	$Fm\,\bar{3}\,c$ (no. 226)
Z	8
a/Å	13.5548 (10)
V/Å^3	2,490.5 (6)
ρ_{calc}/g cm^{-3}	7.32
$\mu_{MoK\alpha}$/cm^{-1}	211.7
Reflections: parameters	187: 11
R_1 ($I > 2\sigma_{(I)}$)[a]	0.0156
R_1 (all data)[a]	0.0165
wR_2 ($I > 2\sigma_{(I)}$)[a]	0.0261
wR_2 (all data)[a]	0.0262
Largest peak; deepest hole/e Å^{-3}	0.45; −0.73[b]

[a]$R_1 = \Sigma\|\|F_o| - |F_c\|\|/\Sigma|F_o|$; $wR_2 = [\Sigma[w(F_o^2 - F_c^2)^2]]/[\Sigma[w(F_o^2)^2]]^{1/2}$, where $w = 1/[\sigma^2 F_o^2 + (0.0032P)^2 + 33.84]$, and $P = (F_o^2 + 2F_c^2)/3$;
[b]The largest peak and the deepest hole are 1.9 Å away from Cd/Li and 0.8 Å away from Cd/Li, respectively.

Paratone-N oil. The measurements were conducted at a temperature of 200 K. Data integration and semiempirical absorption correction were performed with the Bruker-supplied software (Bruker AXS Inc, 2014). The crystal structure was solved with the intrinsic phasing method and was refined with full-matrix least-squares minimization on F^2 using ShelXL (Sheldrick, 2015). Olex2 software was used as a graphical interface (Dolomanov et al., 2009). Atomic coordinates of all compounds reported in this paper were standardized with the Structure Tidy program (Gelato and Parthé, 1987). All sites were refined with anisotropic displacement parameters. Final difference Fourier map was flat and featureless. Selected crystallographic data are summarized in Table 1.

One specific aspect of the refinements concerning the site occupation factors (SOF) requires a special mention. All SOFs were checked by freeing an individual SOF, while other variables were kept fixed. No statistically significant deviations were observed for the SOF of the Ba site (8*a*); the Li position (8*b*) indicated a freely-refined SOF of ca. 105%. The detected "over-occupation" of the Li atom barely had statistical significance (deviations were within ca. 3-4σ). The Cd site (96*i*) showed approximately 94–95% occupancy (within ca. 8-9σ), which is indicative of the existence of either 1) vacancies, or 2) potential disordering with a lighter element, such as Li in this case. The model with Li/Cd co-occupation was chosen on the basis of expected greater electronic structure stability of $BaLi_xCd_{13-x}$ ($x \approx 2$) vs. $BaLiCd_{12-x}$ ($x \approx 0.6$–0.7). We must also note that ignoring the above-mentioned signs for a small disorder on the Cd site (96*i*) and refining an ordered $BaLiCd_{12}$ model leads to a converging least-squares minimization, however, with increased R-values (R_1 = 0.0182; wR_2 = 0.0443) compared to those in presented Table 1 for the $BaLi_xCd_{13-x}$ ($x \approx 2$) structure. Residual difference peak and hole in the Fourier synthesis map were also much higher, therefore, this possibility was excluded from further consideration. Further details of the structural work are discussed later on. The corresponding crystallographic information files (CIF) for $BaLi_xCd_{13-x}$ ($x \approx 2$) and $BaCd_{11}$ have been deposited with CSD, and the data for this paper can be obtained free of charge *via* http://www.ccdc.cam.ac.uk/conts/retrieving.html (or from the CCDC, 12 Union Road, Cambridge CB2 1EZ, United Kingdom; Fax: +44-1223-336033; E-mail: deposit@ccdc.cam.ac.uk). Depository numbers are 2184513 ($BaLi_xCd_{13-x}$) and 2184514 ($BaCd_{11}$).

2.3 Electronic structure calculations

To investigate the chemical bonding of all compositions, electronic structure calculations were performed within the local density approximation (density functional theory) using the TB-LMTO-ASA program (Tank et al., 1994). Experimental unit cell parameters and atomic coordinates obtained in this study were used as the input parameters in our calculation. In order to satisfy the atomic sphere approximation (ASA), we employed von-Barth-Hedin functional (Von Barth and Hedin, 1972) and introduced empty spheres during the calculation. The Brillouin zone was sampled by 1,000 *k*-point grid. Electronic density of states (DOS), atom-projected electronic density of states (PDOS), and crystal orbital Hamilton population (COHP) were calculated with modules in the LMTO program (Steinberg and Dronskowski, 2018).

3 Results and discussion

3.1 Crystal structure

The structures of some AM_{13} compounds (space group $Fm\,\bar{3}\,c$; A = K, Rb, Ca, Sr, Ba and M = Zn, Cd) were first reported by Ketelaar in 1937 (Ketelaar, 1937). The first material synthesized and characterized in this group was $NaZn_{13}$, which has become the archetype of the family (Pearson symbol *cF*112) (Villars and Calvert, 1991). The structure is relatively complex, although there are only three unique positions in the asymmetric unit. For the herein discussed $BaLi_xCd_{13-x}$ ($x \approx 2$), they are listed in Table 2. The overall $NaZn_{13}$ structure is often referred to as cage-like and can be visualized as a face-centered cubic arrangement of snub cubes (Zn1, at site 96*i*) surrounding the Na atoms (at site 8*a*). The third position is taken by a Zn atom (Zn2, at site 8*a*), centering a Zn_{12}-icosahedron (notice the atypical 12-fold Zn2 coordination

TABLE 2 Atomic coordinates and equivalent displacement parameters (Å^2) for $BaLi_xCd_{13-x}$ ($x \approx 2$).

Atom	Wyckoff symbol	Site symmetry	x	y	z	U_{eq}[a]
Ba	8*a*	4 3 2	1/4	1/4	1/4	0.0142 (3)
Cd/Li[b]	96*i*	*m* . .	0	0.11998 (3)	0.17782 (3)	0.0154 (2)
Li	8*b*	$m\,\bar{3}$	0	0	0	0.018 (6)

[a]U_{eq} is defined as one third of the trace of the orthogonalized U_{ij} tensor.
[b]Refined as mixed-occupied Cd/Li in a ratio of 0.905 (4)/0.095.

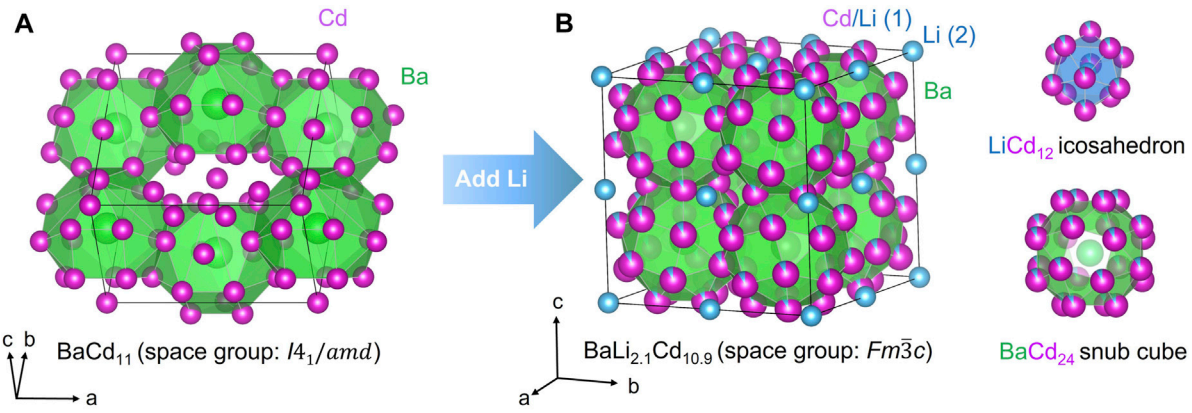

FIGURE 1
(A) $BaCd_{11}$ crystallizes in a tetragonal structure type. It cannot transition to the cubic $NaZn_{13}$ structure even with the presence of excessive Cd. **(B)** $BaLi_{2.1}Cd_{10.9}$ crystallizes in the cubic $NaZn_{13}$ structure type).

by Zn1). A more detailed structural description can be found in Ref (Nordell and Miller, 1999). and Ref. (Häussermann et al., 1998).

There are over a hundred compounds reported to crystallize in the $NaZn_{13}$ structure type (Villars and Calvert, 1991). In the past 2 decades, the $NaZn_{13}$ family has been expanded to include many ternary counterparts, some of which are cubic alloys, such as $EuCu_xAl_{13-x}$ (Phelan et al., 2012) and $RECo_{13-x}Ga_x$ (*RE* = La, Ce, Pr, Nd, and mischmetal) (Weitzer et al., 1990), while some other show crystallographic ordering. Examples of the latter group are $BaLi_7Al_6$ (Häussermann et al., 1998), AM_xT_{13-x} (*A* = Ba, Sr, La, Eu, *M* = Cu and Ag; *T* = Al, Ga and In; x = 5–6.5.) (Nordell and Miller, 1999), ACu_9Tt_4 (*A* = Ca, Sr, Ba, Eu; *Tt* = Si, Ge, Sn) (Schäfer et al., 2012), and $BaAu_xZn_{13-x}$ (Gupta and Corbett, 2012). One should notice that most structurally characterized phases are known to follow the "1-13" stoichiometry, while other members are shown to be slightly off-stoichiometric, such as $SrZn_{13-x}$ (Wendorff and Röhr, 2006), and $EuZn_{13-x}$ (Saparov and Bobev, 2008), where the Zn-deficiency is necessitated for the sake of attaining more favorable valence electron count. More discussion on that topic will follow later. In some cases, particularly among the ternaries, ordering of the elements leads to cubic to tetragonal distortion ($Fm\,\bar{3}\,c$ to $I4/mcm$) as seen on the examples of ACu_9Tt_4 (*A* = Ca, Sr, Ba, Eu; *Tt* = Si, Ge, Sn) (Schäfer et al., 2012), but this is not the case here; the symmetry of $BaLi_xCd_{13-x}$ ($x \approx 2$) is strictly cubic.

We also need to draw attention to the fact that while $BaZn_{13}$ (rather $BaZn_{\sim 12.8}$) is known to crystallize with the cubic $NaZn_{13}$ structure type (Wendorff and Röhr, 2006), a binary compound $BaCd_{13}$ with the said structure does not exist. The most Cd-rich phase is $BaCd_{11}$ and it crystallizes in its own structure type (tetragonal space group $I4_1/amd$ (no. 141); Pearson symbol *tI*48) (Sanderson and Baenziger, 1953). Despite the compositional difference and despite crystallizing in different space groups, the $NaZn_{13}$ and $BaCd_{11}$ structure types share a lot in common in terms of the large polyhedra surrounding the Na and Ba atoms, respectively (Figure 1). In the tetragonal structure, each Ba atom is surrounded by 22 Cd atoms (Cd1), while the Cd2 atoms have 12 nearest neighboring Cd ones. A more comprehensive structural description of the $BaCd_{11}$ structure type can be found in Ref. (Sanderson and Baenziger, 1953). Besides $BaCd_{11}$, $YbZn_{11}$ (Kuzma et al., 1965), $SrCd_{11}$ (Köster and Meixner, 1965), $CeZn_{11}$ (Zelinska et al., 2004), and $PrZn_{11}$ (Iandelli and Palenzona, 1967) are also reported to form with the same structure type.

Apparently, the $NaZn_{13}$ structure can only be stabilized with Ba and Cd only when a small amount of lithium is present, with $BaLi_{2.1}Cd_{10.9}$ being the final refined composition (Table 1). One lithium atom takes over the Zn2 site in the $NaZn_{13}$ prototype structure, while the balance of lithium atoms per formula unit is admixed with Cd at the Zn2 site in a ratio of ca. 1:10 (Table 2). The consequence of the Li atoms being in such positions is that, instead of having the same kind of atoms on both the vertices and the centers of the icosahedra, the center of the 12-membered polyhedron is Li, while the vertices are mostly Cd atoms. We confirmed that the hypothetic cubic $BaCd_{13}$ phase was inaccessible without Li (*vide supra*). In such a Cd-rich environment, the crystals that grow are the tetragonal $BaCd_{11}$. The exact opposite scenario is observed when one moves up in group 12 to Zn—the most Zn-rich phase in the Ba–Zn binary system is the cubic $BaZn_{13}$ (Wendorff and Röhr, 2006)) while tetragonal $BaZn_{11}$ does not exist.

Based on the above and given the similarities between the two structure types, one may ask the question as to what is the role Li atoms play to stabilize the cubic $BaLi_xCd_{13-x}$ ($x \approx 2$) phase, and whether or not the homogeneity range can be expanded. Our experimental findings are limited to compositions close to the refined, and an unambiguous answer to the two questions is not possible at present. However, we can speculate that since most known compounds within the $NaZn_{13}$ structural family show valence electron counts close to $27e^-$ per formula unit (Häussermann et al., 1998; Nordell and Miller, 1999), one should expect, based on electronic arguments alone, that the composition $BaLi_xCd_{13-x}$ ($x \approx 1$) would be preferred. Recognizing that there are geometric factors at play, too, and that they might be in competition with the electronic factors, could lead to different conclusions. In fact, there has been much debate about the favorable conditions of which structure type ($NaZn_{13}$ or $BaCd_{11}$) is optimal, yet, no universal conclusion has been reached. The hard-sphere colloidal model shows that the ideal size ratio between *A* and *M* is between 0.49 and 0.63 (Hachisu and Yoshimura, 1980; Yoshimura and Hachisu, 1983; Bartlett et al., 1992; Shevchenko et al., 2005). Later, Hudson (Hudson, 2010) approached this problem with the optimal packing fraction analysis. It is shown that the majority of the AM_{13} compounds yield a close packing fraction between 0.69 and 0.77. However, multiple known compounds break this rule. A typical example is $SrBe_{13}$ (Matyushenko et al., 1964) yielding a size ratio of 2, which is far from the ideal range mentioned previously. It can be also suggested, again from a purely geometrical perspective, that the size of the atom in the icosahedral environment (recall that the covalent radii of Li and Zn are nearly identical while Li and Cd differ (Pauling, 1960)) is also a contributing factor, and could tip the scales when it comes to the phase-preference between cubic $NaZn_{13}$ vs. tetragonal $BaCd_{11}$.

Therefore, we can argue that the composition $BaLi_xCd_{13-x}$ ($x \approx 2$) may be the limiting/preferred one for the stabilization of the $NaZn_{13}$-type structure for *both* electronic and geometric reasons.

3.2 Electronic structure

The bonding characteristics of $BaLi_{2.1}Cd_{10.9}$ and $BaCd_{11}$ are investigated *via* electronic structure calculations using the LMTO program (Tank et al., 1994). Accurate modeling of the electronic properties of $BaLi_{2.1}Cd_{10.9}$ with the LMTO program is possible, yet challenging, due to the mixed occupancy of Li and Cd on the 96*i* site. The input of the mixed occupancy to the model would only be possible by reducing the cubic symmetry to triclinic *P*1, while assigning corresponding positions to Li and Cd atoms according to the refined occupancy. To simplify the calculation and to avoid symmetry reduction, we evaluated the electronic properties of $BaLi_{2.1}Cd_{10.9}$ in its original symmetry without considering the existence of Li on the Cd site. The model employed was the idealized $BaLiCd_{12}$ compound with an ordered cubic structure, where each Ba, Cd, and Li atom resides on an independent site. Atomic coordinates were taken from Table 2.

The atom-projected electronic density of states (DOS) for $BaLiCd_{12}$ and $BaCd_{11}$ are shown in Figures 2A,C, respectively. For $BaLiCd_{12}$, a dip of the total DOS to ca. Three states eV^{-1} unit $cell^{-1}$ can be observed at around $E–E_F$ = 0.19 eV. In the rigid-band approximation, shifting the Fermi level ca. 0.2 eV would correspond to seven additional electrons per unit cell, or $0.88e^-$ per formula unit. For $BaCd_{11}$, a dip to ~5 eV^{-1} unit $cell^{-1}$ can be observed right near the Fermi level. However, neither are deep enough to be identified as pseudogaps.

In both compounds, the states in the vicinity of the dips are primarily contributed by the s-orbitals of Cd and Ba. Actually, the density of states plots of both compounds exhibit little structuring, with no gaps in the range of $-3\ eV < E–E_F < 9\ eV$. This is the characteristic of metallic bonding, indicating the absence of localized states or lone pairs. It appears that both systems are stabilized by the interaction between the delocalized electrons.

The crystal orbital Hamilton population curves (COHP) for selected averaged interactions in $BaLiCd_{12}$ and $BaCd_{11}$ are plotted in Figures 2B,D. For $BaLi_2Cd_{11}$, the Ba–Cd interactions are under-optimized at the Fermi level, while the Cd–Li and Cd–Cd interactions are almost optimized at the Fermi level. In contrast, for $BaCd_{11}$, all interactions are under-optimized at the Fermi level. The optimized Cd–Li and Cd–Cd bondings in the cubic $BaLiCd_{12}$ compared to the under-optimized bonding in the $BaCd_{11}$ phase could be an indication of higher stability of the former. Given the similarity between the COHP curves of the Ba–Cd contacts in both compounds, the bond strength of Cd–Li and Cd–Cd in the icosahedron might be the driving force of

10.3389/fchem.2022.991625

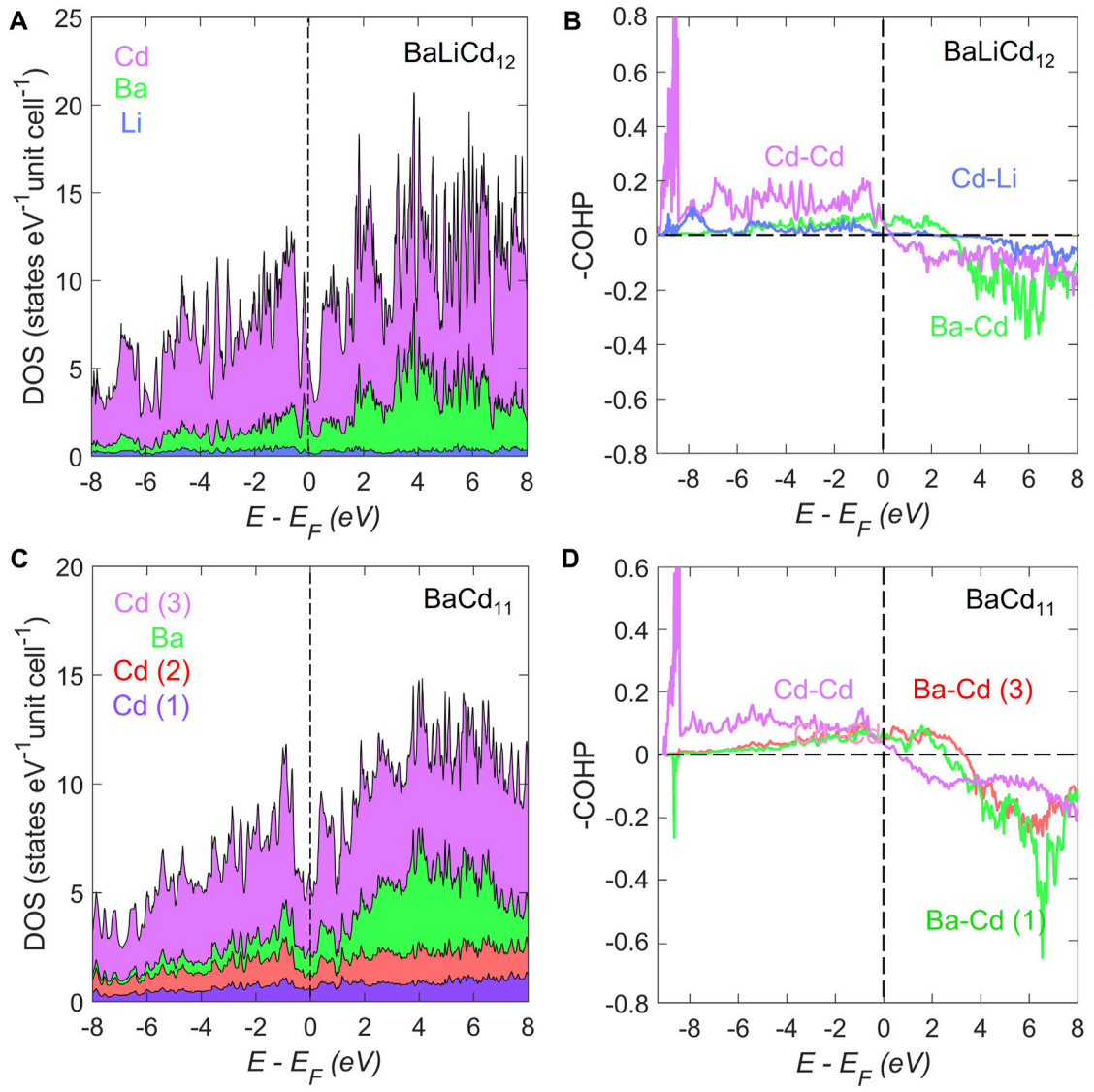

FIGURE 2
The atom-projected electronic density of states (DOS) for **(A)** $BaLiCd_{12}$ and **(C)** $BaCd_{11}$. The DOS of both compounds exhibit characteristics of metallic bonding. A relatively larger dip can be observed in the $BaLiCd_{12}$ compound compared to that of $BaCd_{11}$. The crystal orbital Hamilton population curves (COHP) for the averaged selected interactions of **(B)** $BaLiCd_{12}$ and **(D)** $BaCd_{11}$. For $BaLiCd_{12}$, the Ba–Cd interactions are underoptimized at the Fermi level, while the Cd–Li and Cd–Cd interactions are almost optimized at the Fermi level. In contrast, for $BaCd_{11}$, all interactions are under-optimized at the Fermi level.

the transition between these two phases. This inference is in line with the geometric explanation in the previous subsection.

4 Summary and outlook

The bonding characteristics of the Cd-rich phases, $BaLi_{2.1}Cd_{10.9}$ and $BaCd_{11}$, both made from Cd flux, were studied both experimentally and computationally. In addition to providing insight into the relative stability of the tetragonal $BaCd_{11}$ and cubic $NaZn_{13}$ structures, this study reports the discovery of a new phase $BaLi_{2.1}Cd_{10.9}$, expanding the variety of compounds that crystallize in the $NaZn_{13}$ structure type. Combined with the first-principles calculations of the electronic structure of both phases, we found that the bond strength of Cd–Li and Cd–Cd within the icosahedron might be one of the driving forces leading to the stabilization of the cubic $NaZn_{13}$ type structure in this section of the Ba–Li–Cd phase diagram.

Data availability statement

The datasets presented in this study can be found in online repositories. The names of the repository/repositories and accession number(s) can be found below: The corresponding crystallographic information files (CIF) for $BaLi_xCd_{13-x}$ ($x \approx 2$) and $BaCd_{11}$ have been deposited with CSD, and the data for this paper can be obtained free of charge *via* http://www.ccdc.cam.ac.uk/conts/retrieving.html (or from the CCDC, 12 Union Road, Cambridge CB2 1EZ, United Kingdom; Fax: +44-1223-336033; E-mail: deposit@ccdc.cam.ac.uk). Depository numbers are 2184513 ($BaLi_xCd_{13-x}$) and 2184514 ($BaCd_{11}$).

Author contributions

WP: Investigation, Methodology, Formal analysis, Visualization, Writing—original draft. SB: Conceptualization, Investigation, Formal analysis, Writing—review and editing. SB: Conceptualization, Supervision, Project administration, Writing—review and editing.

Funding

This work received financial support from the National Science Foundation (NSF) through an award number DMR-2004579.

Conflict of interest

The authors declare that the research was conducted in the absence of any commercial or financial relationships that could be construed as a potential conflict of interest.

Publisher's note

All claims expressed in this article are solely those of the authors and do not necessarily represent those of their affiliated organizations, or those of the publisher, the editors and the reviewers. Any product that may be evaluated in this article, or claim that may be made by its manufacturer, is not guaranteed or endorsed by the publisher.

References

Baranets, S., and Bobev, S. (2021a). Caught in action. The late rare earths thulium and lutetium substituting aluminum atoms in the structure of $Ca_{14}AlBi_{11}$. *J. Am. Chem. Soc.* 143, 65–68. doi:10.1021/jacs.0c11026

Baranets, S., Ovchinnikov, A., and Bobev, S. (2021b). Synthesis, crystal and electronic structure of $BaLi_2Cd_2Ge_2$. *Z. fur Naturforsch. B* 76, 689–697. doi:10.1515/znb-2021-0114

Bartlett, P., Ottewill, R., and Pusey, P. (1992). Superlattice formation in binary mixtures of hard-sphere colloids. *Phys. Rev. Lett.* 68, 3801–3804. doi:10.1103/physrevlett.68.3801

Bruker AXS Inc (2014). SAINT.Madison, WI: Bruker AXS Inc.

Dolomanov, O. V., Bourhis, L. J., Gildea, R. J., Howard, J. A., and Puschmann, H. (2009). OLEX2: A complete structure solution, refinement and analysis program. *J. Appl. Crystallogr.* 42, 339–341. doi:10.1107/s0021889808042726

Gelato, L., and Parthé, E. (1987). Structure tidy – A computer program to standardize crystal structure data. *J. Appl. Crystallogr.* 20, 139–143. doi:10.1107/s0021889887086965

Guo, S.-P., Meyers, J. J., Tobash, P. H., and Bobev, S. (2012). Eleven new compounds in the *RE*–Cd–Ge systems (*RE* = Pr, Nd, Sm, Gd–Yb; Y): Crystal chemistry of the RE_2CdGe_2 series. *J. Solid State Chem.* 192, 16–22. doi:10.1016/j.jssc.2012.03.045

Gupta, S., and Corbett, J. D. (2012). $BaAu_xZn_{13-x}$: Electron-poor cubic $NaZn_{13}$-type intermetallic and its ordered tetragonal variant. *Inorg. Chem.* 51, 2247–2253. doi:10.1021/ic2022787

Hachisu, S., and Yoshimura, S. (1980). Optical demonstration of crystalline superstructures in binary mixtures of latex globules. *Nature* 283, 188–189. doi:10.1038/283188a0

Häussermann, U., Svensson, C., and Lidin, S. (1998). Tetrahedral stars as flexible basis clusters in *sp*-bonded intermetallic frameworks and the compound $BaLi_7Al_6$ with the $NaZn_{13}$ structure. *J. Am. Chem. Soc.* 120, 3867–3880. doi:10.1021/ja973335y

Hudson, T. S. (2010). Dense sphere packing in the $NaZn_{13}$ structure type. *J. Phys. Chem. C* 114, 14013–14017. doi:10.1021/jp1045639

Iandelli, A., and Palenzona, A. (1967). Zinc-rich phases of the rare Earth-zinc alloys. *J. Less Common Metals* 12, 333–343. doi:10.1016/0022-5088(67)90001-x

Ketelaar, J. (1937). The crystal structure of alloys of zinc with the alkali and alkaline Earth metals and of cadmium with potassium. *J. Chem. Phys.* 5, 668. doi:10.1063/1.1750098

Köster, W., and Meixner, J. (1965). Der Aufbau der Systeme des Europiums mit Silber, Kadmium und Indium sowie das System Kadmium-Strontium. *Int. J. Mater. Res.* 56, 695–703. doi:10.1515/ijmr-1965-561009

Kuzma, Y. B., Kripyakevich, P., and Frankevich, D. (1965). Compounds of rare-Earth metals with zinc and their crystal structures. *Izvestiia Akademii nauk SSSR Neorganicheskie Mater.* 1, 1547.

Makongo, J. P., Darone, G. M., Xia, S.-Q., and Bobev, S. (2015). Non-stoichiometric compositions arising from synergistic electronic and size effects. Synthesis, crystal chemistry and electronic properties of $A_{14}Cd_{1+x}Pn_{11}$ compounds ($0 \le x \le 0.3$; *A* = Sr, Eu; *Pn* = As, Sb). *J. Mat. Chem. C* 3, 10388–10400. doi:10.1039/c5tc01605c

Matyushenko, N., Verkhorobin, L., and Karev, V. (1964). Strontium beryllide. *Sov. Phys. Crystallogr. Engl. Transl.* 9, 273.

Nordell, K. J., and Miller, G. J. (1999). Linking intermetallics and Zintl compounds: An investigation of ternary trielides (Al, Ga, In) forming the $NaZn_{13}$ structure type. *Inorg. Chem.* 38, 579–590. doi:10.1021/ic980772k

Ovchinnikov, A., and Bobev, S. (2019). Layered quaternary germanides—Synthesis and crystal and electronic structures of $AELi_2In_2Ge_2$ (*AE* = Sr, Ba, Eu). *Inorg. Chem.* 58, 7895–7904. doi:10.1021/acs.inorgchem.9b00588

Pauling, L. (1960). *The nature of the chemical bond*, 260. Ithaca, NY: Cornell University Press.

Phelan, W. A., Kangas, M. J., McCandless, G. T., Drake, B. L., Haldolaarachchige, N., Zhao, L. L., et al. (2012). Synthesis, structure, and physical properties of $Ln(Cu, Al, Ga)_{13-x}$ (*Ln* = La–Pr, and Eu) and $Eu(Cu, Al)_{13-x}$. *Inorg. Chem.* 51, 10193–10202. doi:10.1021/ic301024t

Sanderson, M., and Baenziger, N. (1953). The crystal structure of $BaCd_{11}$. *Acta Crystallogr.* 6, 627–631. doi:10.1107/s0365110x53001745

Saparov, B., and Bobev, S. (2008). Zinc-deficiency in intermetallics with the $NaZn_{13}$ type: Re-Determination of the crystal structure and physical properties of $EuZn_{13-x}$ ($x = 0.25(1)$). *J. Alloys Compd.* 461, 119–123. doi:10.1016/j.jallcom.2007.09.040

Schäfer, M. C., Yamasaki, Y., Fritsch, V., and Bobev, S. (2012). Synthesis and structural characterization of ACu_9Tt_4 (*A* = Ca, Sr, Ba, Eu; *Tt* = Si, Ge, Sn) – tetragonally distorted ternary variants of the cubic $NaZn_{13}$ structure type. Improved structure refinement of $SrCu_2Ge_2$. *Z. Anorg. Allg. Chem.* 638, 1204–1211. doi:10.1002/zaac.201200062

Sheldrick, G. M. (2015). Crystal structure refinement with SHELXL. *Acta Crystallogr. C Struct. Chem.* 71, 3–8. doi:10.1107/s2053229614024218

Shevchenko, E. V., Talapin, D. V., O'brien, S., and Murray, C. B. (2005). Polymorphism in AB_{13} nanoparticle superlattices: An example of semiconductor-metal metamaterials. *J. Am. Chem. Soc.* 127, 8741–8747. doi:10.1021/ja050510z

Steinberg, S., and Dronskowski, R. (2018). The crystal orbital Hamilton population (COHP) method as a tool to visualize and analyze chemical bonding in intermetallic compounds. *Crystals* 8, 225. doi:10.3390/cryst8050225

Suen, N.-T., Huang, L., Meyers, J. J., and Bobev, S. (2018). An unusual triple-decker variant of the tetragonal $BaAl_4$ structure type: Synthesis, structural characterization, and chemical bonding of $Sr_3Cd_8Ge_4$ and $Eu_3Cd_8Ge_4$. *Inorg. Chem.* 57, 833–842. doi:10.1021/acs.inorgchem.7b02781

Tank, R., Jepsen, O., Burkhardt, A., and Andersen, O. (1994). *TB-LMTO-ASA program*. Stuttgart, Germany: Max-Planck-Institut für Festkörperforschung.

Villars, P., and Calvert, L. D. (1991). *Pearson's handbook of crystallographic data for intermetallic phases*. Material Park, OH: ASM.

Von Barth, U., and Hedin, L. (1972). A local exchange-correlation potential for the spin polarized case. i. *J. Phys. C. Solid State Phys.* 5, 1629–1642. doi:10.1088/0022-3719/5/13/012

Wang, J., Yang, M., Pan, M.-Y., Xia, S.-Q., Tao, X.-T., He, H., et al. (2011). Synthesis, crystal and electronic structures, and properties of the new pnictide semiconductors A_2CdPn_2 (A = Ca, Sr, Ba, Eu; Pn = P, As). *Inorg. Chem.* 50, 8020–8027. doi:10.1021/ic200286t

Weitzer, F., Hiebl, K., Grin, Y. N., Rogl, P., and Nöel, H. (1990). Magnetism and structural chemistry of $RECo_{13-x}Ga_x$ alloys (RE = La, Ce, Pr, Nd, and mischmetal *MM*). *J. Appl. Phys.* 68, 3504–3507. doi:10.1063/1.346362

Wendorff, M., and Röhr, C. (2006). Polar binary Zn/Cd-rich intermetallics: Synthesis, crystal and electronic structure of $A(Zn/Cd)_{13}$ (A = alkali/alkaline Earth) and $Cs_{1.34}Zn_{16}$. *J. Alloys Compd.* 421, 24–34. doi:10.1016/j.jallcom.2005.11.016

Xia, S.-Q., and Bobev, S. (2006). $Ba_{11}Cd_8Bi_{14}$: Bismuth zigzag chains in a ternary alkaline-Earth transition-metal Zintl phase. *Inorg. Chem.* 45, 7126–7132. doi:10.1021/ic060583z

Xia, S.-Q., and Bobev, S. (2007). Cation-anion interactions as structure directing factors: Structure and bonding of Ca_2CdSb_2 and Yb_2CdSb_2. *J. Am. Chem. Soc.* 129, 4049–4057. doi:10.1021/ja069261k

Xia, S.-Q., and Bobev, S. (2007). Synthesis, structural characterization, electronic structure, and magnetic properties of the Zintl phase $Eu_{10}Cd_6Bi_{12}$. *Chem. Asian J.* 2, 619–624. doi:10.1002/asia.200700016

Xia, S.-Q., and Bobev, S. (2006). Temperature-dependent crystallographic studies and electronic structure of $Ba_2Cd_3Bi_4$. *J. Solid State Chem.* 179, 3371–3377. doi:10.1016/j.jssc.2006.07.003

Yoshimura, S., and Hachisu, S. (1983). "Order formation in binary mixtures of monodisperse lattices," in *Front. Colloid. Sci. In memoriam professor dr. Bun-ichi Tamamushi Progress in Colloid and Polymer Science* (Berlin, Germany: Springer), Vol. 68, 59–70.

Zelinska, O., Conrad, M., and Harbrecht, B. (2004). Refinement of the crystal structure of cerium zinc (1:11), $CeZn_{11}$. *Z. Kristallogr. - New Cryst. Struct.* 219, 389–390. doi:10.1524/ncrs.2004.219.14.389

Zürcher, F., Wengert, S., and Nesper, R. (2001). Crystal structure of barium dimagnesium dilithium disilicide, $BaLi_2Mg_2Si_2$, and of barium dimagnesium dilithium digermanide. $BaLi_2Mg_2Ge_2$. *Z. Kristallogr. - New Cryst. Strct.* 216, 503. doi:10.1524/ncrs.2001.216.14.537